Gas-and liquid-phase reactions on sulphated zirconia prepared by precipitation

S. Melada[a], M. Signoretto[a,*], F. Somma[a], F. Pinna[a], G. Cerrato[b], G. Meligrana[b], and C. Morterra[b]

[a]*Department of Chemistry, University of Venice, Calle Larga S. Marta 2137, I-30123 Venice, Italy (INSTM Consortium – UdR Venice)*
[b]*Department of Chemistry IFM, University of Turin, Via P. Giuria 7, I-10125 Turin, Italy (INSTM Consortium – UdR Turin)*

Received 2 December 2003; accepted 19 February 2004

Sulphated zirconia (SZ) was synthesized under different precipitation and ageing conditions. Catalysts were characterized by nitrogen adsorption–desorption, thermal analysis, FTIR and Raman spectroscopy. The catalytic performance of these SZ systems in both gas and liquid-phase reactions has been investigated. The effect of precipitation and ageing conditions has been studied and a correlation with catalytic activity has been tried.

KEY WORDS: sulphated zirconia; anisole acylation; pore size distribution.

1. Introduction

Liquid-phase reactions, such as Friedel–Crafts acylation [1], are important unit processes for the preparation of many industrially valuable chemicals. Traditionally, these reactions have been conducted using stoichiometric amount of liquid Brnsted acids (such as H_2SO_4) or Lewis acids (such as $AlCl_3$ or BF_3). Nowadays the restrictions imposed by the waste minimization laws and economic considerations drive to the development of a new catalytic technology. Modern processes are, in fact, based on solid acids. In particular, sulphated zirconia (SZ) has been shown to be active for a number of reactions [2,3] including isomerization [4–7], cracking [8], alkylation [9–12] and also Friedel–Crafts acylation [13–20].

A good heterogeneous catalyst for liquid-phase reactions must possess, besides active catalytic sites, a pore structure capable to host large reagents and to allow the formation of the desired products.

The goal of our work is therefore to synthesize SZ catalysts with different texture and to test these catalysts in two different reactions: (i) the gas-phase isomerization of *n*-butane and (ii) the liquid-phase acylation of anisole.

The former reaction involves small reactants and products. The latter one concerns large molecules and diffusion limitations. In this latter case, both structural and textural properties of the catalyst should play a key role in determining the final activity. For this reason, we prepared a series of SZ samples by modulating, in the synthesis, the parameters influencing the textural properties of the final catalyst, namely the precipitation pH and the ageing conditions.

* To whom correspondence should be addressed.
E-mail: miky@unive.it

2. Experimental

2.1. Catalysts synthesis

Catalysts were prepared via two different conventional precipitation methods. In the first one [21], $ZrOCl_2 \cdot 8H_2O$ was dissolved in distilled water and added dropwise under vigorous stirring to an ammonia solution. During the entire course of the precipitation, the pH value was kept constant at 8 or 10 by the continuous addition of a 10N ammonia solution. In the second method, instead, 10N ammonia solution was added dropwise into the zirconyl chloride solution until the pH reached the target value. In both cases, after the complete addition of the salt solution, the hydroxide suspension was aged for 20 h either at room temperature (*K* series), or at 90 °C under reflux conditions (*R* series) [22]. The aged hydroxides were filtered and washed with distilled water until they were free from chloride ions ($AgNO_3$ test).

The samples were dried at 110 °C and then impregnated with $(NH_4)_2SO_4$ by an incipient wetness method. The nominal sulphates loading was 8% $SO_4^{=}$ by weight. All samples were then calcined at 650 °C for 3 h in flowing air.

Samples have been labelled as follows: (*R* or *K*) (*v* or *c*) *n* where *R* stays for refluxed samples and *K* for non-refluxed ones. The precipitation pH was indicated by *n*, with *v* for variable and *c* for constant pH. For example, the refluxed sample precipitated at constant pH 10 was labelled as Rc10.

2.2. Catalysts characterization

Surface area and pore size distribution were obtained from N_2 adsorption/desorption isotherms at −196 °C (Micromeritics ASAP 2000 Analyser). Surface area was calculated from the adsorption branch by the BET equation, whereas the pore size distribution was

1011-372X/04/0500–0193/0 © 2004 Plenum Publishing Corporation

determined by the BJH method also applied on the adsorption isotherm [23].

Thermal analyses were performed on a NETZSCH STA 409C instrument in flowing air with temperature rate set at 10 °C/min in the 25–800 °C temperature range. Sulphate content was determined by a previously described ion chromatographic method [24].

Insitu FTIR spectra were obtained on a BRUKER 113v spectrophotometer (2 cm^{-1} resolution, MCT detector). SZ-based samples were inspected in the form of thin layer deposition (~10 mg cm^{-2}) on Si wafers, starting from aqueous solutions. All samples were activated in controlled atmosphere at 400 °C in quartz cells (equipped with KBr windows) connected to a gas vacuum line, equipped with rotary and turbomolecular pumps (residual pressure $p < 10^{-5}$ Torr).

Raman spectra were obtained at 4 cm^{-1} resolution using a FRA 106/RFS 100 FT Bruker spectrophotometer, equipped with Nd/YAG laser (Near IR emission and variable power in the 0–300 mW range) and with a Ge detector (D-418-S).

CO chemisorption measurements were carried out at 30 °C (i.e. RT) using a Micromeritics ASAP 2010 analyser on SZ samples activated *in vacuo* at the desired temperature.

2.3. Catalytic tests

2.3.1. Catalysts were tested in two different reactions

The gas-phase isomerization of *n*-butane was carried out at atmospheric pressure at 150 and 250 °C by feeding 25 mL/min of reaction mixture (n-C_4H_{10}/He = 1/4 at 150 °C; n-$C_4H_{10}/H_2 = 1/4$ at 250 °C). Before reaction, all catalysts (500 mg) were activated in dry airflow (50 mL/min) at 450 °C for 90 min. The products were analysed on-line by an HP-6890 gas chromatograph equipped with a TCD detector [25].

The liquid-phase reaction (acylation of anisole with benzoyl chloride) was carried out as reported in [15,39] at 60 °C in a thermostated batch reactor, using benzoyl chloride (2.65 mmol), anisole (12 mL) and *n*-tetradecane (employed as internal standard for GC). Anisole was distilled under sodium wire before the use and kept over sodium in an inert atmosphere. Benzoyl chloride was kept in a dry box. Before the introduction in the reaction medium, the catalyst (200 mg) was activated at 450 °C in flowing air for 1 h and kept dry. After 3 h the reaction mixture was quickly cooled down, separated from the catalyst and analysed on a HP-6890 gaschromatograph equipped with HP-5 column and a FID detector. GC-MS measures were conducted in order to recognize the methoxybenzophenone isomers.

3. Results and discussion

The surface characterization results are reported in table 1. All isotherms obtained by N_2 adsorption at liquid nitrogen temperature relative to calcined samples belong to type IV IUPAC classification, with hysteresis loop of type H2-H3 (figure 1). The precipitation procedure at pH 10 leads to samples characterized by higher surface area than those obtained by precipitation at pH 8. When the ageing step is carried out under reflux conditions the surface area shifts to very high values, as also reported in the (recent) literature concerning this subject [22,26–29]. Surface areas of uncalcined refluxed samples are very high, especially for those synthesized at pH 10 (300–450 m^2/g), whereas those of non-refluxed samples are smaller (200–250 m^2/g). During calcination, there is an impressive drop of surface area (see table 1). This decrease in surface area is mirrored by important modifications both in the bulk and at the surface of the samples, as indicated by thermal analysis data (see below), with a different behaviour from one series to the other.

The BJH pore size distributions were calculated on the adsorption branch of nitrogen isotherms (inset in figure 1). Pore dimensions are in the mesoporous range for all the calcined samples. Pore size distributions are wider and shifted to higher mean values for refluxed samples than for the non-refluxed ones. It is worth noting that: (i) SZ samples precipitated at pH 10 possess larger pores if compared with samples obtained at pH 8; (ii) the ageing process under reflux favours the develop-

Table 1
Surface characterization data for calcined samples

Sample	Surface area (m^2/g)		Pore volume (mL/g)	Mean pore diameter (Å)	$SO_4^{=}$ content (wt%)	$SO_4^{=}$ density (groups/ nm^{-2})	Phase composition after calcination (f_T)[a]
	Before calcination	After calcination					
Rc10	442	122	0.32	104	4.32	2.22	70.0
Rv10	419	112	0.23	81	3.83	2.15	65.0
Kc10	270	89	0.12	53	3.62	2.54	55.4
Rc8	337	106	0.16	60	3.90	2.31	65.3
Rv8	270	93	0.12	50	3.56	2.40	–
Kc8	229	82	0.09	46	3.31	2.54	72.8

[a]% *t*-ZrO_2 obtained on the basis of the equation proposed by Evans *et al.* [P.A. Evans, R. Stevens and J.G.P. Binner, Br. Ceram. Trans. J., 83 (1984) 39].

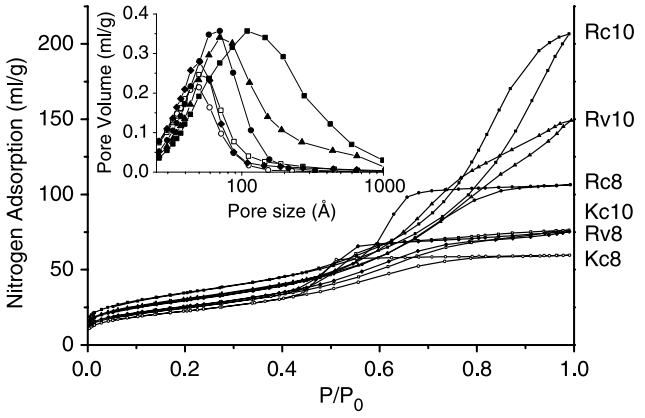

Figure 1. N_2 adsorption/desorption isotherms of all the samples. Inset: BJH pore size distribution calculated on the adsorption branch of the N_2 isotherm. Rc10: ■; Rv10: ▲; Kc10: □; Rc8: ●; Rv8: ◆; Kc8: ○.

ment of a network of very large pores characterized by a wide size distribution. This feature can be explained in terms of pore wall collapse during calcination. In fact, refluxed uncalcined samples possess a very broad pore size distribution (data not reported for the sake of brevity) with a considerable contribution from mesoporosity if compared to non-refluxed uncalcined systems, which, in turn, are mostly microporous. The calcination brings about the collapse of micropores to form larger pores, whereas crystallization induces the toughening of pore walls. Refluxed hydroxides exhibit, in addition to the micropores collapse phenomenon [27], a broadening of the existing mesopores network.

For calcined systems the sulphate content data show that refluxed samples retain more sulphur than non-refluxed ones. This points out that there is an increase in the sulphate retention parallel to the surface area growth (see table 1). But, if we normalize the sulphate content per surface area unit (i.e. as $SO_4^{=}/nm^2$) we can observe that the sulphate spreading is almost the same for all the samples, ranging in the half-monolayer sulphates coverage [30].

Some DTG/DTA profiles are shown in figure 2. For each sample we can roughly divide the explored temperature range into four regions: the first one, from 50 to 250 °C, is dominated by an endothermic, broad peak, most likely ascribable to the loss of water by about 9–12%wt. There are remarkable differences among the various samples. DTG curves of Rc10 and Kc10 uncalcined systems show a similar behaviour, as these samples loose a large amount of water at ~110–120 °C, with a second smaller weight loss at higher temperature (peak centred at ~200 °C). Rv10 sample shows the first weight loss peak at ~150 °C, whereas Rc8 sample starts loosing water at the highest temperature (peak centred at ~170 °C). The second region ranges from 250 to 500 °C and no substantial modifications are evident for all samples. In this region, there is only a slight weight loss (3–5%), due to the decomposition of the sulphating

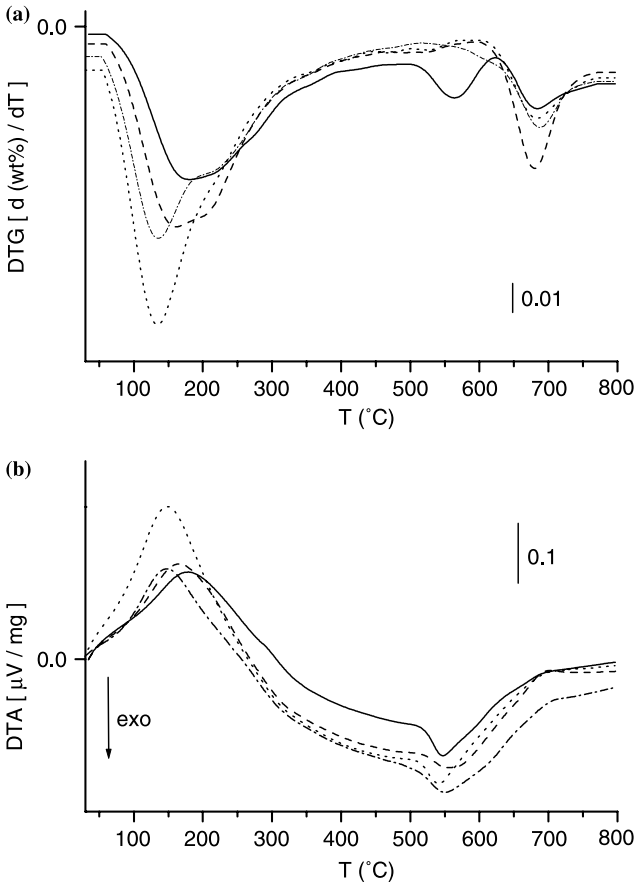

Figure 2. (a) DTG curves of some uncalcined samples. (b) DTA profiles of the same samples. Rc10: dotted line; Rv10: dashed line; Kc10: dash-dot line; Rc8: solid line.

agent (ammonium sulphate) with loss of ammonia and NO_x. The third region (from 500 to 600 °C) is dominated by an exothermic peak, most likely ascribable to the amorphous-to-crystalline transition process of the $Zr(OH)_4$ starting system. It must be recalled that when the crystallization process takes place in the presence of anionic species, like sulphates, the ZrO_2 tetragonal modification is favoured [31] and the transition shifts to higher temperature, whereas in the absence of stabilizing species, the ZrO_2 monoclinic modification is the standard thermodinamically stable phase. It is note worthy, that the Rc8 sample shows in this region an anomalous weight loss (~2%) which can be probably due to a structure modification (dehydroxylation) process. The corresponding non-refluxed Kc8 sample (data not reported) shows no recordable weight loss in the same region. The fourth and last region lies between 600 and 800 °C: in this range, the typical weight loss peak associated to the sulphate species decomposition (endothermic) is often overlapped with the ZrO_2 polymorphic transition to the thermodynamically stable monoclinic phase (exothermic). The weight loss in this region lies in the 3.5–4.5% range.

As we can observe, the sulphates decomposition takes place at about the same temperature for all the samples

(DTG peak centred around 670–680 °C). This seems to indicates that there is only a negligible contribution from the surface structure modification on the sulphate decomposition.

As for the spectral characterization of surface functionalities (sulphates, in this specific case), some data relative to FTIR spectroscopy are reported in figure 3a. All spectra have been obtained after activation *in vacuo* at 400 °C, in order to reproduce roughly the activation treatment which is carried out prior to the catalytic tests. The spectral profiles of surface sulphates brought to a medium–high dehydration stage relative to both Kc10 and Kc8 samples indicate that these materials possess a medium-to-large fraction of monoclinic ZrO_2 phase, as witnessed by the presence in the 1150–850 cm^{-1} range of figure 3 of several components due to slightly different $-_{S-O}$ stretching modes [32]. On the contrary, Rc10, Rv10 and Rc8 samples present (almost) only a sharp $-_{S-O}$ component that is normally ascribed to the presence of the ZrO_2 tetragonal modification. This is further confirmed by Raman spectroscopy (figure 3b) and by X-ray diffraction data (not reported for the sake of brevity). In fact, the spectral profiles of *K* specimens (in particular Kc10) show peaks ascribable to both monoclinic and tetragonal modifications of ZrO_2, whereas bands of m-ZrO_2 are (almost) totally absent for the all R systems.

Samples precipitated at pH 10 and aged under reflux conditions are less crystalline than the corresponding non-refluxed ones and, in fact, they show small peaks in the Raman spectra. This is due to the fact that refluxed samples are microcrystalline, as Risch and Wolf displayed [29]. If the ageing step is accomplished under reflux conditions at high pH (>9) [28] the precipitated hydrous zirconia can undergo dissolution and reprecipitation. The reprecipitated crystallites are smaller in size than those in the original precipitate. During calcination, the sintering process that takes place among the particles causes the growth of the crystallites, but it affects the refluxed samples to a lesser extent.

After this characterization step, all the samples were examined in both of the above mentioned reactions. The gas-phase isomerization reaction gave the following results: at 150 °C in helium all catalysts deactivate rapidly, as already observed [33–35], whereas at 250 °C in hydrogen flow, after an initial steep decrease of activity (from 45 to 50% *n*-butane conversion to 20–23% after the first hour on stream) all samples reach a steady conversion after about 3 h (200 min - t.o.s.). Catalytic runs were followed for about 20 h but no further changes happened during this period of time. Steady conversion is 19–20% for the pH 10 precipitated samples and 16–17% for the samples precipitated at pH 8. The ageing step seems to have a minimal influence on the activity behaviour of the samples.

The activity towards this reaction, as claimed elsewhere [24,36–38], depends mainly on the acid strength of the catalyst, which in turn is influenced by a number of other variables, like, for instance, sulphates content and type, hydration degree, crystallinity, crystal defects and phase composition.

These variables are difficult to control by the synthesis parameters: in the present case, it seems that the sulphate spreading is a dominating factor in determining the catalytic activity. In table 1, we can see that the sulphate surface density (expressed as $SO_4^{=}$ groups/nm^2) is much the same for all catalysts, the refluxed samples having only a slightly lower value than conventionally prepared samples, due to their higher surface area.

We observe now the performance of our catalysts in the liquid-phase acid-catalysed acylation of anisole (scheme 1). As we know, anisole reacts with benzoyl chloride (acylating agent) on the catalyst surface to give the corresponding ketone, either 2- or 4- methoxybenzophenone (2- and 4-MBP) and HCl. The only GC-detectable side reaction is the decomposition of benzoyl chloride with water to give benzoic acid (scheme 2). Water could be present as a solvent impurity. A trace amount of phenyl benzoate could indicate that benzoic acid further reacted in a very small amount with anisole or maybe phenol (produced by hydrolysis of anisole). Our catalysts show very good selectivity towards MBP ketones, its value reaching 89% for the best catalyst. The *ortho* : *para* ratio reaches the value of 3:97, slightly higher than that of the homogeneously catalysed reac-

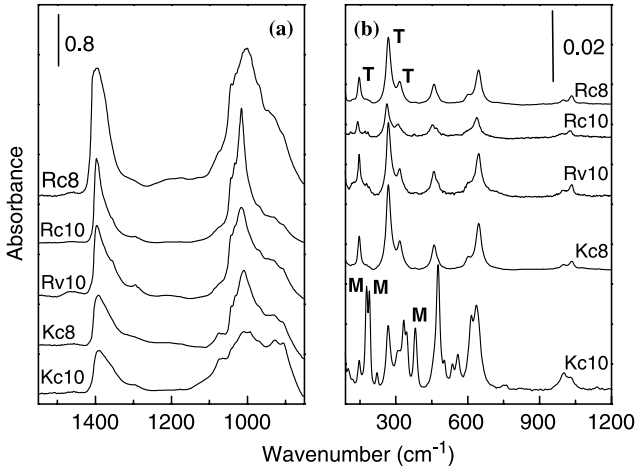

Figure 3. (a) IR spectral profile of surface sulphates for some refluxed and non-refluxed samples activated *in vacuo* at 400 °C; (b) Raman spectra of the same samples of section a.

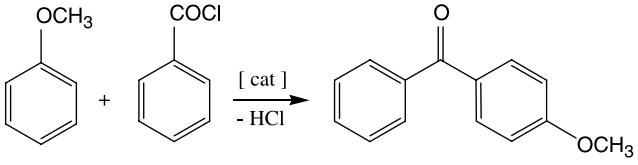

Scheme 1. Acylation of anisole with benzoyl chloride.

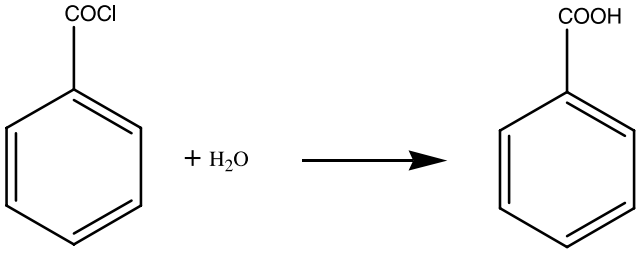

Scheme 2. Decomposition (hydrolysis) of benzoyl chloride.

tion (5:95) reported by Kemnitz and co-workers. [39]. Our measures were reproducible with an error of less than 5%.

Benzoyl chloride conversion, after 3 h batch reaction, and selectivity towards the desired products and their yields are collected in table 2. It is possible to observe that conversions tend to be higher for refluxed than for non-refluxed samples. Moreover, pH 8 samples show lower conversions than for the pH 10 ones. Selectivity is usually high (>80%) for quite all the samples. Samples Rv10 and Kc10 have the lowest selectivity (benzoyl chloride is decomposed to a high extent for these catalysts).

In figure 4, we try a correlation between benzoyl chloride conversion and pore distribution or surface area (inset). It can be seen that conversion grows fast with average pore size. The maximum value is observed for the Rc10 sample, followed by the other refluxed (*R*) catalysts. Non-refluxed samples (*K*) do not show remarkable differences of pores size and, consequently, of conversion. It can also be observed that catalytic data correlate quite well with the surface areas, mainly the ones of the constant pH samples. A similar trend could be drawn from the sulphate content. As these results make clear, it is necessary to use mesoporous materials to have considerable conversions in a liquid medium reaction (at moderate temperatures), in which bulky molecules (both reagents and products) have to diffuse into and/or through the catalyst pores. For example, Rc10 sample (average pore diameter ~100 Å) converts

Table 2
Catalytic test data

Sample	Conversion of BCL (%)	Selectivity Σ MBP (%)	Yield Σ MPB (%)	Steady state conversion of n-butane (%)
Rc10	46	89	40	19.5
Rv10	45	71	32	18.5
Kc10	35	75	26	20.1
Rc8	40	88	35	16.5
Rv8	34	82	27	16.1
Kc8	34	85	29	16.4

Acilation: conversion of benzoyl chloride, selectivity and yield of 2- and 4-methoxybenzophenone after 3 h batch test at 60 °C. Isomerization: steady-state conversion of *n*-butane at 250 °C in H_2 flow (after 20 h t.o.s.)

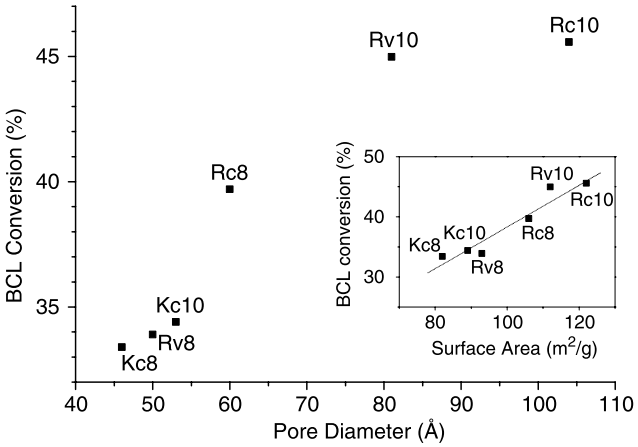

Figure 4. Acylation of anisole with benzoyl chloride after 3 h at 60 °C as a function of pore diameter and surface area (inset).

80% of the benzoyl chloride after 20 h at 60 °C with a MBP yield of more than 60%, whereas Kc10 (average pore diameter ~50 Å) converts only the 60% of the reagent with a MBP yield of 50%.

It is now desirable to know if the differences in the textural properties, which affect so much the acylation reaction but not at all the isomerization activity, have a similar effect on the surface acidity. In order to make this feature clear, FTIR spectroscopy of the adsorption/desorption of suitable probe molecules (like, for instance, CO and 2,6-dimethylpyridine (2,6-DMP)) has been resorted to test surface acidity. In particular: (i) the adsorption/desorption of CO at RT has been employed to reveal the strong fraction of Lewis acid sites present on the catalysts, whereas (ii) the adsorption/desorption of 2,6-DMP at both RT and 150 °C has been used to test the total, Lewis and Brnsted, acidity of the powders.

It is known that CO is a weak Lewis base and, when adsorbed at RT like in the present case, it is able to evidence only the strongest fraction of Lewis acid sites, giving rise to a band centred at ~2200 cm^{-1} (ν_{CO} with respect to the free gaseous molecule ~ +55–60 cm^{-1}) [40].

CO adsorption measurements were carried out onto the various SZ samples. Even if FTIR spectra are not quantitatively reliable, the adoption of strictly constant experimental conditions allowed us to observe that no remarkable differences exist among the various systems, but for a slight difference in the intensity of the CO bands and a certain difference of spectral position and band form achieved by the ν_{CO} bands. This latter aspect deserves some attention, as the SZ samples aged in non-refluxing conditions seem to exhibit the typical spectral behaviour of CO adsorbed at the surface of (mainly) monoclinic ZrO_2 systems (e.g., see [40]). This feature so confirms the presence of the monoclinic ZrO_2 phase at the surface of the *K* systems.

Volumetric chemisorption measurements have been carried out on some of the SZ samples in order to ascertain the quantitative aspects of CO uptake.

The results obtained for CO adsorption at 300 K (not reported for the sake of brevity) allows us to conclude that the (minor) spectroscopic differences observed only derive from the different scattering properties of morphologically different SZ samples.

As far as the surface total acidity is concerned, the adsorption of 2,6-DMP has been employed. In fact, this probe possesses a strong basic character and is able to evidence both Lewis and Brnsted acid sites, giving rise to specific bands in the 1700–1500 cm^{-1} (~1580–1616 cm^{-1} when Lewis-bound, and ~1625–1660 cm^{-1} when Brnsted-bound) [41].

On the basis of the spectral behaviour (not reported) and of literature data [42], we observed that the adsorption of 2,6-DMP gives rise to bands due to the presence of both Lewis and Brnsted acidity.

If we compare the spectroscopic information with those from sulphate analysis we can conclude that, at least on a qualitative ground, the surface acidity is similar for all SZ samples, either prepared by the reflux method or obtained by a conventional ageing process. This indicates that the different catalytic activity in one of the two processes explored depends primarily on the (surface) structure and pore size distribution of the catalysts.

4. Conclusions

We found that SZ prepared by hydroxide precipitation at different pH and ageing conditions exhibits remarkable differences in the textural and bulk properties but a similar sulphate spreading (similar acidities). At the same time, they do not show valuable differences in the isomerization of *n*-butane. This is probably due to the similar acid strength of all samples, because the molecules engaged in this gas -phase reactions are small. Little differences in the catalytic activity are only ascribable to the different precipitation pH and not to the ageing step. Unlike that, the liquid-phase acylation of anisole with benzoyl chloride requires also a highly mesoporous pore network, in order to allow the diffusion of the large molecules involved. As a consequence, the acylation activity of the SZ systems of similar acid strength turned out to depend appreciably on the pore size distribution of the catalyst.

Acknowledgment

We wish to thank Dr. Marta Pellizon Birelli for her kindness in doing the thermal measurements.

References

[1] J.H. Clark and D.J. Macquarrie, Org. Proc. Res. Dev. 1 (1997) 149.
[2] K. Tanabe and W.F. Hölderlich, Appl. Catal. A 181 (1999) 399.
[3] G.D. Yadav and J.J. Nair, Micropor. Mesopor. Mater. 33 (1999) 1.
[4] M. Hino and K. Arata, J. Chem. Soc., Chem. Commun. 851 (1980).
[5] T. Yamaguchi, Appl. Catal. A 61 (1990) 1.
[6] K. Arata, Adv. Catal. 37 (1990) 165.
[7] T. Yamaguchi, Appl. Catal. A 222 (2001) 237.
[8] B.H. Davis, R.A. Keogh and R. Srinivasan, Catal. Today 20 (1994) 219.
[9] C. Guo, S. Yao, J. Cao and Z. Qian, Appl. Catal. A 107 (1994) 229.
[10] G.D. Yadav and T.S. Thorat, Ind. Eng. Chem. Res. 35 (1996) 721.
[11] J.H. Clark, G.L. Monks, D.J. Nightingale, P.M. Price and J.F. White, J. Catal. 193 (2000) 348.
[12] G.D. Yadav, P.K. Goel and A.V. Joshi, Green Chem. 3 (2001) 92.
[13] M. Hino and K. Arata, J. Chem. Soc., Chem. Commun. 112 (1985).
[14] K. Arata and M. Hino, Appl. Catal. 59 (1990) 197.
[15] V. Quaschning, J. Deutsch, P. Druska, H.-J. Jiclas and E. Kemnitz, J. Catal. 177 (1998) 164.
[16] Y. Xia, W. Hua and Z. Gao, Catal. Lett. 55 (1998) 101.
[17] G.D. Yadav and A.A. Pujari, Green. Chem. 1 (1999) 69.
[18] K. Arata, H. Nakamura and M. Shouji, Appl. Catal. A 197 (2000) 213.
[19] J. Deutsch, V. Quashning, E. Kemnitz, A. Auroux, H. Ehwald and H. Lieske, Top. Catal. 13 (2000) 281.
[20] V. Quashning, A. Auroux, J. Deutsch, H. Lieske and E. Kemnitz, J. Catal. 203 (2001) 426.
[21] P. Canton, R. Olindo, F. Pinna, G. Strukul, P. Riello, M. Meneghetti, G. Cerrato, C. Morterra and A. Benedetti, Chem. Mater. 13 (2001) 1634.
[22] M.A. Risch and E.E. Wolf, Appl. Catal. A 172 (1998) L1.
[23] S.J. Gregg and K.S.W. Sing, *Adsorption, Surface Area and Porosity, 2nd ed.* (Academic Press, 1982) p. 111.
[24] C. Sarzanini, G. Sacchero, F. Pinna, M. Signoretto, G. Cerrato and C. Morterra, J. Mater. Chem. 5 (1995) 353.
[25] M. Signoretto, F. Pinna, G. Strukul, P. Chies, G. Cerrato, S. Di Ciero and C. Morterra J. Catal. 167 (1997) 522.
[26] G.K. Chuah, S. Jaenicke, S.A. Cheong and K.S. Chan, Appl. Catal. A 145 (1996) 267.
[27] G.K. Chuah, S. Jaenicke and B.K. Pong, J. Catal. 175 (1998) 80.
[28] K.T. Jung and A.T. Bell, J. Mol. Catal. A 163 (2000) 27.
[29] M.A. Risch and E.E. Wolf, Appl. Catal. A 206 (2001) 283.
[30] P. Nascimento, C. Aktatopoulou, M. Oszagyan, G. Coudrier, C. Travers, J.F. Joly and J.C. Vedrine, in: New Frontiers in Catalysis, eds. L. Guczi, F. Solymosi and P. Tetenyi (Elsevier Science Publisher B.V., 1993) p. 1185.
[31] R.C.J. Garvie, J. Phys. Chem. 39 (1965) 1238.
[32] M. Waquif, J. Bachelier, O. Saur and J.C. Lavallay, J. Mol. Catal. 72 (1992) 127.
[33] F. Pinna, M. Signoretto, G. Strukul, G. Cerrato and C. Morterra, Catal. Lett. 26 (1994) 339.
[34] D. Spielbauer, G.A.H. Mekhemer, E. Bosch and H. Knözinger, Catal. Lett. 36 (1996) 59.
[35] S.Y. Kim, J.G. Goodwin Jr. and D. Galloway, Catal. Today 63 (2000) 21.
[36] C. Morterra, G. Cerrato, F. Pinna and M. Signoretto, J. Catal. 157 (1995) 109.
[37] C. Morterra, G. Cerrato, G. Meligrana, M. Signoretto, F. Pinna and G. Strukul, Catal. Lett. 73 (2001) 113.
[38] C. Morterra, G. Cerrato, F. Pinna, M. Signoretto and G. Strukul, J. Catal. 149 (1994) 181.
[39] K. Parida, V. Quaschning, E. Lieske and E. Kemnitz, J. Mater. Chem. 11 (2001) 1903.
[40] C. Morterra, G. Cerrato, C. Emanuel and V. Bolis, J. Catal. 142 (1993) 349.
[41] C. Morterra, G. Cerrato and G. Meligrana, Langmuir 17 (2001) 7053.
[42] C. Morterra, G. Meligrana, G. Cerrato, V. Solinas, E. Rombi and M.F. Sini, Langmuir 19 (2003) 5344.